Multi-directional Assessment of Respiratory and Cardiac Pulsatility of the Inferior Vena Cava From Ultrasound Imaging in Short Axis

Ultrasound in Med. & Biol., Vol. ■, No. ■, pp. ■■■–■■■, 2020

0301-5629/$ - see front matter

https://doi.org/10.1016/j.ultrasmedbio.2020.08.027

● *Technical Note*

MULTI-DIRECTIONAL ASSESSMENT OF RESPIRATORY AND CARDIAC PULSATILITY OF THE INFERIOR VENA CAVA FROM ULTRASOUND IMAGING IN SHORT AXIS

Luca Mesin,* Paolo Pasquero,† and Silvestro Roatta‡

* Mathematical Biology and Physiology, Department of Electronics and Telecommunications, Politecnico di Torino, Torino, Italy; † Department of Medical Sciences, University of Torino, Torino, Italy; and ‡ Integrative Physiology Lab, Department of Neuroscience, University of Torino, Torino, Italy

(*Received* 22 *May* 2020; *revised* 29 *July* 2020; *in final from* 30 *August* 2020)

Abstract—The pulsatility of the inferior vena cava (IVC) reflects the volume status of patients. It can be investigated by ultrasounds (US), offering an important non-invasive tool supporting fluid management. However, the method has limitations attributable to many confounding factors, *e.g.,* related to IVC movements and non-regular shapes. Short- or long-axis views have been used, both having advantages and limitations in counteracting such confounding factors, depending on the specific condition. The aim of this study is to investigate IVC pulsatility in the different directions on the transverse plane and to assess its variability. Moreover, different components of this pulsatility (induced by either respiratory or cardiac activity) are investigated. The method is tested on 10 healthy patients, with large variations across them of IVC section (mean diameters in the range 1 cm to 3 cm), shape and pulsatility (average caval index [CI] ranging from approximately 20% to 70%). The average coefficient of variation of the CI estimated on 10 different directions was 13% (21% and 20% for the respiratory and cardiac components, respectively), with a range that was approximately 50% of the mean CI across different directions (approximately the same for the 2 different components). The minimum and maximum CI were found close to the directions of maximum and minimum IVC diameter, respectively. The investigation of IVC dynamics in the entire cross-section is crucial to obtain a more repeatable and reliable characterization of IVC pulsatility. The calculation of a CI based on the "equivalent" diameter (proportional to the square root of the IVC cross-sectional area) is encouraged. (E-mail: luca.mesin@polito.it)

Key Words: **Inferior vena cava, Ultrasound, Tracking, Pulsatility, Fluid volume assessment.**

INTRODUCTION

The assessment of blood volume status is an important and challenging issue in emergency medicine, critical care and internal medicine because both hypovolemia and fluid overload can lead to poor clinical outcomes, including prolonged mechanical ventilation, high mortality, renal dysfunction and impairment in oxygenation (Alsous et al. 2000; Murphy et al. 2009; Boyd et al. 2011).

Ultrasound (US) examination of the inferior vena cava (IVC) is a commonly used approach for the assessment of volume status attributable to its non-invasiveness. In particular, the caval index (CI) was demonstrated to correlate with the central venous pressure (Nagdev et al. 2010; Mesin et al. 2019a; Albani et al. 2020), the volume depletion attributable to blood loss, which was studied in blood donors (Pasquero et al. 2015), and the hydration state of patients, so that it could support the management of fluid therapy in critically ill patients (Zhang et al. 2014).

However, the assessment of IVC dynamics is affected by many limitations and confounding factors that impact its accuracy and ultimately its clinical usefulness. Fortunately, modern image processing techniques may help to address and solve some of these limitations and improve repeatability of the measurements (Mesin et al. 2019b). In recent reports, we have proposed semi-automated techniques that improve the reliability of IVC assessment based on the longitudinal approach (long axis), introducing the following new features:

Address correspondence to: Luca Mesin, Dipartimento di Elettronica e Telecomunicazioni, Politecnico di Torino, Corso Duca degli Abruzzi, 24 - 10129 Torino, Italy. E-mail: luca.mesin@polito.it

- Tracking of the IVC, aimed at reducing the artifacts introduced by IVC displacements with respiration (Blehar et al. 2012; Mesin et al. 2015; Mesin et al. 2019c);
- Calculation of the IVC pulsatility over the entire IVC length rather than over a single arbitrary section (Mesin et al. 2019c); and
- Isolation of the respiratory and cardiac components of IVC pulsatility, the latter being potentially more robust and less affected by the spontaneous variability of the respiratory pattern (Sonoo et al. 2015).

Because of anatomic constraints or different habits, in addition to or alternatively to the longitudinal approach, echographers may visualize the IVC in the transverse plane, *i.e.,* in the short axis, (Moreno et al. 1984; Blehar et al. 2009; Chen et al. 2010; Nakamura et al. 2013; Finnerty et al. 2017; Karami et al. 2017; Karami et al. 2018). Also, this approach is affected by the following specific limitations:

- Respiration-related IVC displacement in the mediolateral direction may occur and affect the measurements (Blehar et al. 2012; Mesin et al. 2015; Mesin et al. 2019c);
- One single diameter of the IVC is monitored, but the IVC often exhibits a non-circular cross-sectional shape with different pulsatility along the different directions (Blehar et al. 2012); and
- As observed in longitudinal IVC monitoring (Mesin et al. (2019b), cardiac and respiratory pulsatile components asynchronously interact and increase the variability of IVC pulsatility.

The aim of this study is thus to address many of the limitations affecting the assessment of IVC dynamics in the transverse plane. We present a new methodology for the assessment of the variability of the CI during spontaneous breathing using an automated method that detects the IVC cross-sectional border and measures the pulsatility along all directions. In addition, the analysis is extended to the oscillatory components of cardiac and respiratory origin.

MATERIALS AND METHODS

Subject selection

Included in the study were 10 healthy volunteers (5 females, 5 males; age, mean ± standard deviation 27 ± 7 y; BMI 21 ± 2). The experiments were conducted after the approval by the Ethics Committee of the University of Turin, Italy, on 23 March 2015, in accordance with the Declaration of Helsinki. All patients provided written informed consent for the collection of data and subsequent analysis.

Experimental setup

Participants were supine on a clinical table. Echographic images were obtained using the US system Mylab25 (Gold ESAOTE; Genova, Italy) equipped with a 2-5 MHz convex probe. The upper part of IVC was visualized in subxiphoid or right lateral subcostal position, accounting for anatomic landmarks such as the diaphragm and the portal vein.

The acquisition of US video clips (30-s duration) was taken during spontaneous breathing, 30 min after a participant lay supine on the clinical table.

ANALYSIS

Video processing

A software algorithm (implemented in MATLAB R2019b; MathWorks, Natick, MA, USA) was used to process the short-axis US acquisitions of the IVC. The method detailed later in this report was selected among various techniques, after tests on different data (also including issues such as collapsing IVCs, aberrant cross-sections, artifacts)t: he global thresholding (Otsu 1979) was able to rapidly identify the lumen of the IVC in optimal conditions, but it failed in the case of shadowing artifacts; the active contour (Kass et al. 1988) was computationally intensive, unstable to some US artifacts and it required the choice of parameters to be adapted to the specific condition. Our method was the most stable, allowing the processing of the largest number of US video clips, either in physiology (Folino et al. 2017) or in clinical studies (Pasquero et al. 2020). Moreover, it has a low computational cost, opening [redacted] the perspective of a future real-time implementation. The parameters discussed later in this report were selected on the basis of about 200 US video clips recorded under various conditions (*e.g.,* in terms of patient anatomy and pathology, US acquisition system, setup, *etc.*) and processed in the last year.

The physical dimension of a pixel was determined as a preliminary step by automatically scanning a graduated length scale, present in the US frames. The operator was then asked to select the position of the IVC on the first frame of the video, indicating its center and a rectangle including it. Subsequent image processing considered only a rectangular region with the same dimension, centered on the IVC estimated on the previous frame (thus, tracking the movements of the vein, as detailed later in this report).

Specifically, the following processing was applied on each frame of the video clip in turn. The frame was converted from red, green, blue to a gray-scale (8-bit encode) and cropped on the rectangular region (Fig. 1, a). The contrast was then enhanced using histogram equalization (Fig. 1, b). Next, the image was processed with a 2-D median filter, working on neighborhoods of

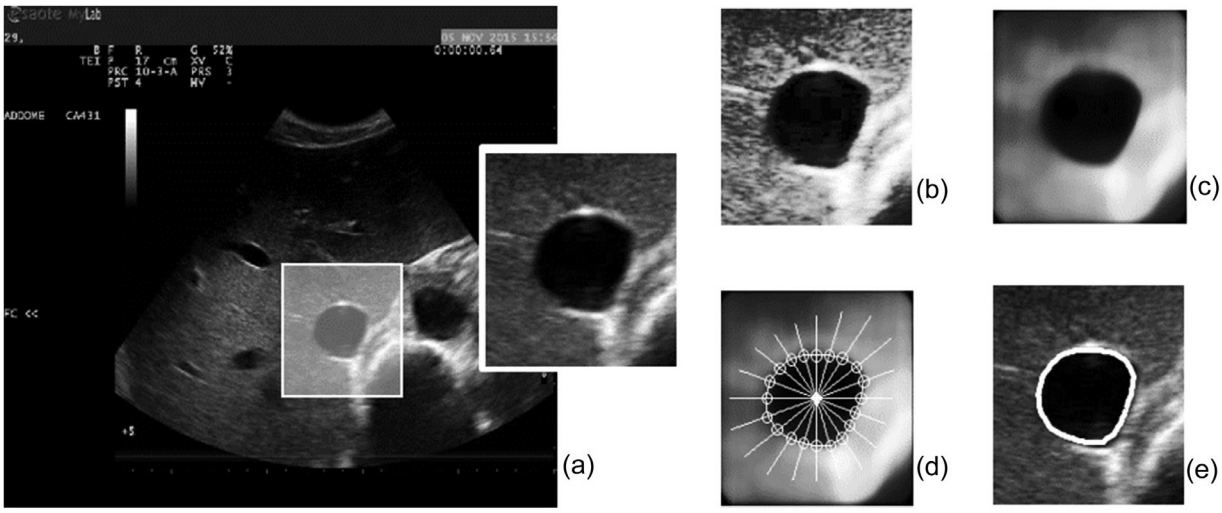

Fig. 1. Processing of a single US frame. (a) A rectangular region is selected. The portion of image is (b) equalized and (c) filtered (by a median filter). (d) The border of the vein is identified along 20 directions, beginning from the IVC centers (from which 10 diameters are obtained), getting (e) the vein boundary (superimposed here to the original portion of image).

11-by-11 pixels (Fig. 1, c). This large smoothing was selected to achieve stable results even when considering low-quality US video clips recorded from patients in emergency conditions. We expect that a smaller neighborhood could also fit well the healthy patients considered here, but we preferred to maintain the same method in our various studies. The outline of the vein was then estimated, its centroid was computed and was used to center the subsequent frame (thus, allowing us to track the vein movements in the medio-lateral direction).

Specifically, the outline of the vein was estimated along 20 equidistant rays, which originated from the center of the considered rectangular portion of the image. The intensity of the pixels along each ray was estimated by cubic interpolation sampling at 100 points. The border of the vein was set where an abrupt increase in intensity was detected, separating a dark and a light region. Specifically, the following ideal assumption was considered: the interior of the vein is dark, with an approximately constant low value of intensity; whereas the exterior is light, with quite a constant high value of intensity (thus, the IVC border separates the dark from the light region). This assumption was considered to estimate the position of the IVC border along a ray, making the following steps.

1. Different points along the ray were considered as potential locations of the border: 10 sampling points before and after the location of the border in the previous frame (except for the first frame, in which the entire ray was explored).
2. The intensity along the ray was approximated by a step function, with a small value in the interior of the vein and a higher one in the exterior. Specifically, for each point selected in step 1, the mean of the intensities of samples before and after it were chosen to approximate the intensity in the interior and exterior of the vein, respectively.
3. The root mean squared errors in approximating the intensity along the ray with these step functions were computed. The border of the IVC was estimated as the point of discontinuity of the step function guaranteeing the best fit of the intensity profile.

To achieve a smooth boundary of the vein, once the 20 border points were found (Fig. 1, d), their spatial coordinates were low pass filtered (Butterworth non-causal, zero-phase IIR spatial filter of order 4 with cut-off at 0.3). The filter was applied to the X and Y coordinates of the border points. Notice that the cut-off frequency is non-dimensional, as already discussed time-series were considered as numeric values with unitary non-dimensional sampling interval. The parameters of the filter were chosen after a fine tuning on few data. Furthermore, the displacement of the vein was assumed to be smooth and small across successive frames: specifically, the maximum variation of the border location along a ray was imposed to be 5 pixels. The border points that overcame such a threshold were considered as outliers and were removed, substituting their value by a quadratic interpolation of the 4 closest neighboring border points.

Post processing

Once the vein boundary was determined (Fig. 1, e), the area of the IVC lumen was numerically computed, summing the contributions of the 20 circular sectors

delimited by pairs of the rays that were discussed earlier in this report. The IVC area was estimated for each frame. Thus, a time series was obtained with a sampling frequency equal to the video frame rate, which was between 11 Hz and 19 Hz (depending on the settings of the US device: the greater the depth and the lower the frame rate).

The signal was then low-pass filtered with a cut-off frequency of 4 Hz (Butterworth non-causal, zero-phase IIR filter of order 4). The cut-off frequency was sufficiently high to preserve cardiac and respiratory components (with a bandwidth of about 1 Hz and some 10th of Hz, respectively).

The effects of the heartbeat and of respiration on the IVC cross-section were then separated using a zero-phase Butterworth filter of order 4 with cut-off frequency of 0.4 Hz. The cardiac and respiratory components were above and below such a cut-off, respectively.

Quantitative measurements

Various indexes were estimated from the IVC diameters along different directions and from the area time series. Concerning the area time series, an equivalent diameter was calculated as follows:

$$D = 2\sqrt{\frac{A}{\pi}} \tag{1}$$

Where A indicates the estimated area of the vein. This variable is meant to provide a term of comparison with other studies in the literature, where a single IVC diameter is considered. The local maxima and minima of the equivalent diameter were computed to estimate the CI as follows:

$$CI = \frac{\max(D) = \min(D)}{\max(D)} \tag{2}$$

The CI was computed considering either the whole signal or specific components (*i.e.,* the cardiac or the respiration component). Specifically, the following indexes were considered, as presented in Figure 2.

- The CI, obtained considering the entire signal during a single respiratory cycle. The respiratory cycles were automatically identified on the respiratory component. The software then explored the entire signal on 1-s windows centered on each local maxima and minima of the respiratory component and searched for maxima or minima to estimate the extension of the pulsation.
- The respiratory caval index (RCI), considering only the respiratory component on a single breath cycle, computed for each respiratory cycle in the video clip.
- The cardiac caval index (CCI), obtained considering subsequent local extremes in the diameter time series, for the most part induced by a single heartbeat (one measurement was obtained for each cardiac cycle in the video clip). This index was not statistically different from the CI estimated from the cardiac component of the IVC pulsatility. Indeed, the respiratory component was quite slow, marginally affecting the local extremes reflecting a single cardiac pulsation.

CI, RCI and CCI were computed for each cycle in a video clip (either respiratory cycle or heartbeat) and then averaged. A representative example of the use of the equivalent diameter is presented in Figure 2. Then, as we are interested in demonstrating the variability of the estimations along different directions, the pulsatility indexes were also computed for each of the 10 diameters considered (obtained from the 20 rays originated from IVC center used for the recognition of the edge of the vein).

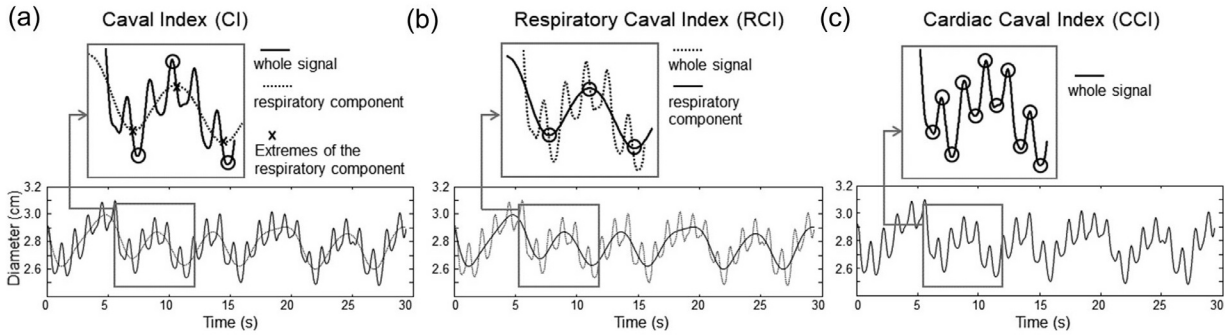

Fig. 2. (a) Caval index (CI) estimated on the whole signal. The respiratory component is isolated with a low-pass filter and superimposed to the entire signal. Then the maxima and minima of the respiratory component are found. The software automatically explored a window (of duration 1 s) centered in each of these points and saved the local maxima or minima, found on the entire signal (*circles*). (b) Respiratory caval index (RCI), computed on the respiratory component. The respiratory component is isolated with a low-pass filter and superimposed to the whole signal. Maxima and minima, automatically found on the respiratory component and used for RCI calculation (*circles*). (c) Cardiac caval index (CCI) computed processing the entire signal. Maxima and minima, automatically found on the whole signal and used for CCI calculation, are presented.

RESULTS

Figure 3 presents the range of variation of the IVC cross-section during a period of 30 s. Note that relative changes vary in the different directions (Figs. 3, a and b). This implies that the CI measurement is considerably affected by the direction investigated (Fig. 3, c). Also notice that, in the average, the pulsatility is larger along the directions in which the vein has a small extension (*i.e.,* minimum diameter) than along that of maximum size.

Figure 4 presents the distributions (in terms of median, quartiles and range) of CI, RCI and CCI estimated from each subject, considering different diameters (*i.e.,* different directions). The estimated borders of the veins are presented at the bottom of Figure 4—irregular shapes were found. Notice that round IVCs (*e.g.,* patients 1, 4, 5) are usually associated with lower values of CI (possibly indicating that they are kept circular by a higher internal pressure) than those with a flat shape (patients 2, 3, 6, 7, 10). The indexes vary a good amount along different directions. On average, the pulsatility indexes had a coefficient of variation (defined as standard deviation divided by the mean value, considering for each subject the estimates from different diameters) equal to 13% for CI, 21% for RCI and 20% for CCI. Notice that the coefficients of variation of the CCI are quite high, similar to those of RCI, even if the range is low, which is attributable to the low mean values of the CCI. As also presented in Figure 3, the measure of pulsatility can vary a good amount over different directions. Thus, an average value of the diameter is suggested to reduce the variance of the estimation and to provide an overall indication of the dynamics of the vein.

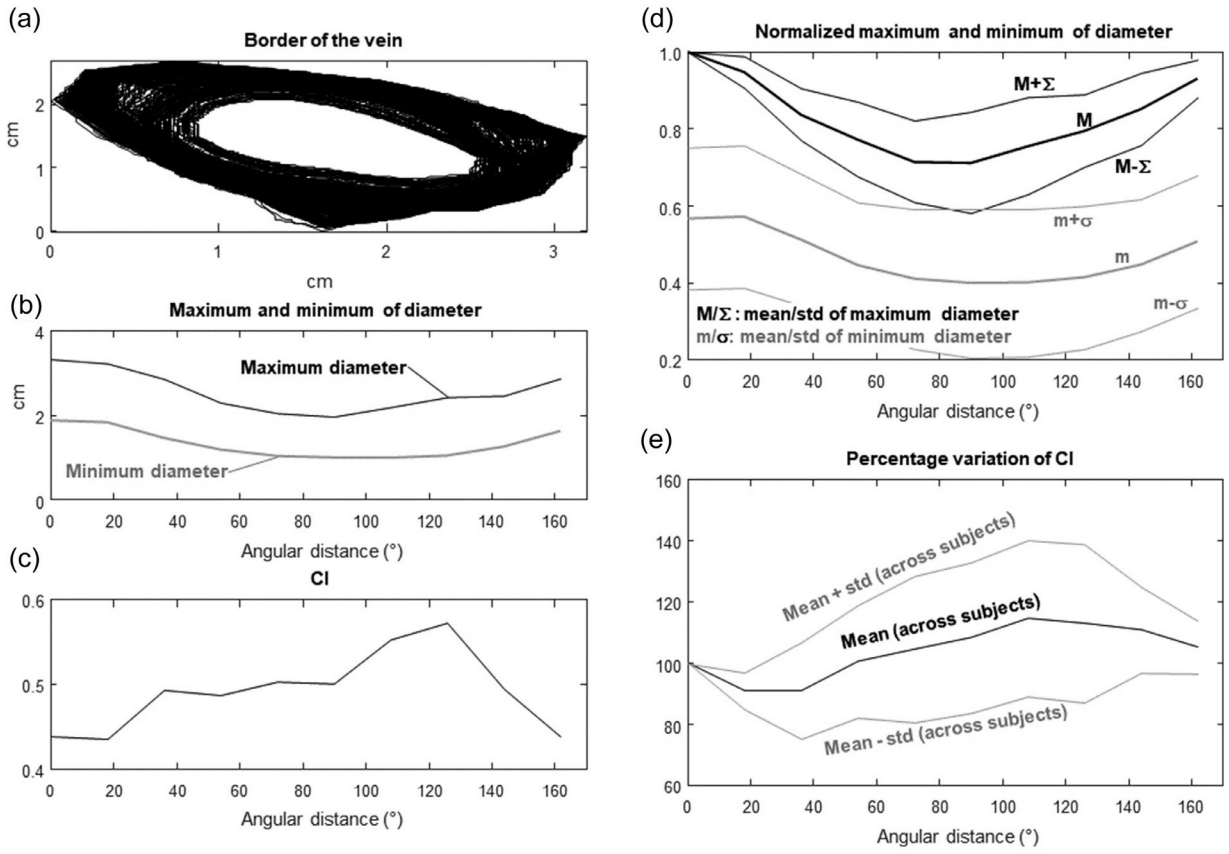

Fig. 3. Maximal and minimal diameters along different directions and corresponding CI computed by the standard method, *i.e.,* considering the whole signal (the angles are measured starting from the direction along which the maximal diameter was found). (a) Border of the IVC for a specific subject (the borders of all 373 frames are presented). (b) Maximal and minimal diameters for the same representative subject as in (a), as a function of the angular distance with respect to the direction along which the maximal diameter was found. (c) Caval index obtained from the data in (b). (d) Average and mean ± standard deviation of maximal and minimal diameters across different patients, normalized with respect to the maximum diameter. (e) Percentage variation of the caval index (average and mean ± standard deviation across patients) computed from different sections of the vein (angle of 0° corresponds to the direction of the maximum diameter).

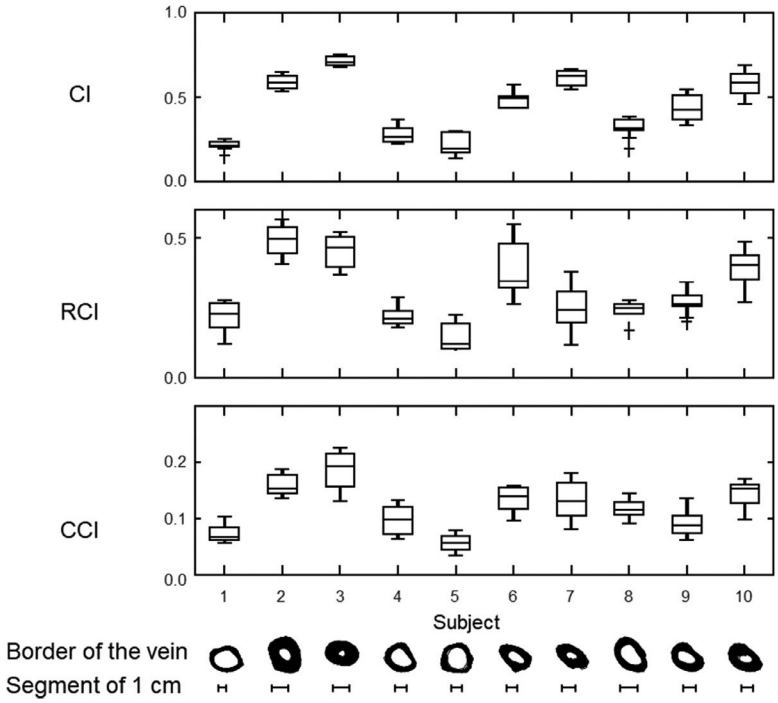

Fig. 4. Values of CI, RCI and CCI evaluated on 10 diameters for each subject. The central mark is the median, the edges of the box are the 25th and 75th percentiles, the whiskers extend to the most extreme data points (not considering outliers, individually indicated). On average, the coefficient of variation (averaging across angles) was 13% for CI, 21% for RCI and 20% for CCI. At the bottom of the Figure, the identified borders of the IVC are presented (superposition of all traces obtained for all frames).

DISCUSSION

In this report, we addressed some of the limitations that affect the estimation of CI in short axis and introduced technical and methodologic improvements oriented to reduce their effect on the measurement, namely the following:

- By means of a semi-automated detection and tracking of the IVC, the in-plane movements of the vein can be accounted for and the movement-related artifacts virtually eliminated (the IVC movements in the longitudinal direction cannot be eliminated using a short-axis view, instead);
- The averaging of the IVC size and pulsatility over all possible directions yields univocal and non-subjective measurements; and
- The identification and quantification of the magnitude of cardiac and respiratory components of IVC pulsatility may possibly help to account for a major confounding factor related to the intrinsic variability of spontaneous respiration.

However, our method is still affected by some intrinsic problems of IVC investigation in short axis, *e.g.,* the lack of control of longitudinal displacements and the possibility that the insonation plane is not orthogonal to the IVC axis and changes during the acquisition. Thus, our results are still operator dependent, even if some of the problems of the standard measurement along a single direction have been addressed. The use of multi-planar US imaging, with orthogonal directions to record both the short and long axes, together with tracking algorithms for the two views (*e.g.,* Mesin et al. [2019c] for the long axis and the proposed method here for the short axis) could be of help to compensate in part for these problems.

The tracking of the IVC was proven effective in the improvement of accuracy in assessing CI in the long-axis view (Mesin et al. 2015; Sonoo et al. 2015; Mesin et al. 2019c). However, the IVC exhibits respiratory-related movements also in the short axis, which are in the order of 4 mm (Blehar et al. 2012). Albeit small, this displacement may produce relevant alterations in the antero-posterior diameter assessed in M-mode, *e.g.,* in the order of 8.5% in a hypothetical circular IVC of 20-mm diameter, but the effect may considerably increase in non-circular or smaller veins. Preliminary results of this method have been presented by Folino et al. (2017) in which the IVC was tracked for the investigation of the effects of isometric respiratory efforts, during apnea of short duration.

Other methods for IVC tracking in the short axis have also been proposed in the literature (Nakamura et al. 2013;

Bellows et al. 2014; Karami et al. 2017; Karami et al. 2018). We also tested a few of these approaches in a preliminary phase, which were shown to have a higher computational cost and to be more sensitive to some US artifacts, with respect to the finally adopted method. Specifically, a simple thresholding algorithm was sensitive to hypo-echoic bands (or "dark shadows"). An active contour—"snake"—(discussed by Kass et al. (1988) could also be attracted by a dark artifact. Moreover, we found it difficult to select parameters to fit different conditions (*e.g.,* video clips with different contrasts or IVCs with different shapes/dimensions, and hence curvatures). Assuming constraints to stabilize the estimations (*e.g.,* that the IVC is about circular or ellipsoidal) could limit the applicability of the algorithm. Indeed, the IVC of hypovolemic patients could have aberrant shapes (*e.g.,* it could even be not convex, thus being much different from an ellipse) or even collapse in some frames. Based on many trials and errors, the present algorithm was selected as the most stable against the huge variability of IVC shapes and dynamics, specifically found in patients (Pasquero et al. 2020, unpublished data).

Moreover, our algorithm presents a low computational cost, with the available implementation in MATLAB (MathWorks), which interpreted single core implementation, run on a personal computer with an Intel Core i7-2630 QM, Quad-Core (Intel Corporation, Santa Clara, CA, USA) clock frequency of 2 GHz, 6 GB of RAM and 64-bit operating system). Processing a frame took an average of shorter than 150 ms. As the bandwidth of the processed data is of a few Hz, the actual implementation is almost adequate for a real-time application, which, together with the feedback provided by the rendering of the estimated IVC border, could guide the echographers to acquire an optimal video clip. Moreover, such a potential future implementation could provide to the operator an immediate indication of the pulsatility indexes.

IVC pulsatility is commonly assessed through the CI, which is based on the measurement of maximum and minimum diameters. However, the diameter is an ambiguous definition when the cross-sectional shape of IVC is considerably different from a circle, which is often the case in patients who are hypovolemic or have low central venous pressure (Huguet et al. 2018). Moreover it has been reported that IVC exhibits anisotropic deformation both in response to blood volume changes (Murphy et al. 2009) and during spontaneous breathing (Blehar et al. 2012), with larger diameter changes along the minor axis (according to an elliptical approximation). Here, we have explored the IVC pulsatility along 10 different directions and confirm that the larger pulsatility approximately occurs close to the direction in which the vein presents a smaller diameter (Figs. 3, d and e). In addition, the results point out that, depending on the patient, the CI may vary considerably with the direction, *e.g.,* in subject number 5 maximum CI is about twice the minimum (Fig. 4, *top*). This indicates that measuring along a single direction, whether arbitrarily chosen by the operator or imposed by the US machine, would not provide a representative indication of the global IVC behavior and would thus impair reliability of the assessment (*e.g.,* limiting the possibility of assessing precisely the volume condition of a patient or of scheduling the follow-up of a patient during a treatment for fluid management). Conversely, averaging over all different directions provides a more representative and less operator-dependent indication of IVC collapsibility.

Because the initial observations (reported in Nakamura et al. 2013) that cardiac pulsatility can be detected in IVC and used to monitor changes in volume status, a number of studies explored this possibility (Sonoo et al. 2015; Folino et al. 2017; Mesin et al. 2019a; Mesin et al. 2019c; Albani et al. 2020). Although it is generally considered that the CI quantifies the respiratory-induced changes in IVC diameter, the present results further emphasize the concept that the cardiac component contributes substantially to the overall pulsatility. In fact, the isolated respiratory component yields RCI values that are markedly smaller than the corresponding CI (Fig. 4). The results reported in Figure 4 also demonstrate that all three indexes (CI, RCI and CCI) exhibit some dependence on the considered direction. However, they demonstrate good qualitative agreement in the characterization of the different patients. Considering that the intrinsic variability of spontaneous respiration, in terms of depth of respiratory acts and in dependence of the type of breathing (thoracic versus abdominal involvement), is considered to be a major source of variability of IVC assessment (Muller et al. 2012; Folino et al. 2017), the observations discussed earlier support the idea that CCI could be adopted as a surrogate of CI, with the relevant advantage of being virtually independent of respiratory activity; however, notice that some interaction is expected between RCI and CCI, as higher cardiac pulsations are expected during the respiration phase in which the IVC is less full.

Notice that the present results were collected on healthy patients. In certain clinical conditions, *e.g.,* with hypovolemic patients, the IVC cross-sectional shape may be considerably distorted (Huguet et al. 2018), which would amplify the differences in IVC size and pulsatility along the different directions. In that situation, a global assessment of IVC size and pulsatility would be even more beneficial.

CONCLUSIONS

We have introduced an innovative method that identifies the cross-section of IVC from US video clips, and analyzes IVC pulsatility along multiple directions,

separating the cardiac from the respiratory component. The considerable variation of IVC pulsatility along different directions points out the limitation of relying on a single, arbitrary direction and indicates that a global assessment of IVC size and pulsatility may improve objectivity and reliability of the measurement.

Conflict of Interest/Disclosure—An instrument implementing the algorithm described in this report was patented by Politecnico di Torino and Universita di Torino (WO 2018/134726).

REFERENCES

Albani S, Pinamonti B, Giovinazzo T, de Scordilli M, Fabris E, Stolfo D, Perkan A, Gregorio C, Barbati G, Geri P, Confalonieri M, Lo Giudice F, Aquaro G, Pasquero P, Porta M, Sinagra G, Mesin L. Accuracy of right atrial pressure estimation using a multi-parameter approach derived from inferior vena cava semi-automated edge-tracking echocardiography: A pilot study in patients with cardiovascular disorders. Int J Cardiovasc Imaging 2020;36:1213–1225.

Alsous F, Khamiees M, DeGirolamo A, Amoateng-Adjepong Y, Manthous C. Negative fluid balance predicts survival in patients with septic shock: A retrospective pilot study. Chest 2000;117:1749–1754.

Bellows S, Smith J, Mcguire P, Smith A. Validation of a computerized technique for automatically tracking and measuring the inferior vena cava in ultrasound imagery. Stud Health Technol Inform 2014;207:183–192.

Blehar D, Dickman E, Gaspari R. Identification of congestive heart failure *via* respiratory variation of inferior vena cava diameter. Am J Emerg Med 2009;27:71–75.

Blehar D, Resop D, Chin B, Dayno M, Gaspari R. Inferior vena cava displacement during respirophasic ultrasound imaging. Crit Ultrasound J 2012;4:18.

Boyd J, Forbes J, Nakada T, Walley K, Russell J. Fluid resuscitation in septic shock: A positive fluid balance and elevated central venous pressure are associated with increased mortality. Crit Care Med 2011;39:259–265.

Chen L, Hsiao A, Langhan M, Riera A, Santucci K. Use of bedside ultrasound to assess degree of dehydration in children with gastroenteritis. Acad Emerg Med 2010;17:1042–1047.

Finnerty N, Panchal A, Boulger C, Vira A, Bischof J, Amick C, Way D, Bahner D. Inferior vena cava measurement with ultrasound: What is the best view and best mode?. West J Emerg Med 2017;18:496–501.

Folino A, Benzo M, Pasquero P, Laguzzi A, Mesin L, Messere A, Porta M, Roatta S. Vena cava responsiveness to controlled isovolumetric respiratory efforts. J Ultrasound Med 2017;36:2113–2123.

Huguet R, Fard D, d'Humieres T, Brault-Meslin O, Faivre L, Nahory L, Dubois-Rande J, Ternacle J, Oliver L, Lim P. Three-dimensional inferior vena cava for assessing central venous pressure in patients with cardiogenic shock. J Am Soc Echocardiogr 2018;31:1034–1043.

Karami E, Shehata M, Smith A. Segmentation and tracking of inferior vena cava in ultrasound images using a novel polar active contour algorithm. IEEE Global Conference on Signal and Information Processing (GlobalSIP). Piscataway, NJ. : IEEE; 2017. p. 745–749.

Karami E, Shehata MS, Smith A. Estimation and tracking of ap-diameter of the inferior vena cava in ultrasound images using a novel active circle algorithm. Comput Biol Med 2018;98:16–25.

Kass M, Witkin A, Terzopoulos D. Snakes: Active contour models. Int J Comput Vis 1988;1:321–331.

Mesin L, Albani S, Sinagra G. Non-invasive estimation of right atrial pressure using the pulsatility of inferior vena cava. Ultrasound Med Biol 2019;45:1331–1337.

Mesin L, Giovinazzo T, D'Alessandro S, Roatta S, Raviolo A, Chiacchiarini F, Porta M, Pasquero P. Improved repeatability of the estimation of pulsatility of inferior vena cava. Ultrasound Med Biol 2019;45:2830–2843.

Mesin L, Pasquero P, Albani S, Porta M, Roatta S. Semi-automated tracking and continuous monitoring of inferior vena cava diameter in simulated and experimental ultrasound imaging. Ultrasound Med Biol 2015;41:845–857.

Mesin L, Pasquero P, Roatta S. Tracking and monitoring of pulsatility of a portion of inferior vena cava from long axis ultrasound imaging. Ultrasound Med Biol 2019;45:1338–1343.

Moreno F, Hagan A, Holmen J, Pryor T, Strickland R, Castle C. Evaluation of size and dynamics of the inferior vena cava as an index of right-sided cardiac function. Am J Cardiol 1984;53:579–585.

Muller L, Bobbia X, Toumi M, Louart G, Molinari N, Ragonnet B, Quintard H, Leone M, Zoric L, Lefrant J, AzuRea group. Respiratory variations of inferior vena cava diameter to predict fluid responsiveness in spontaneously breathing patients with acute circulatory failure: Need for a cautious use. Crit Care 2012;16:R188.

Murphy C, Schramm G, Doherty J, Reichley R, Gajic O, Afessa B, Micek S, Kollef M. The importance of fluid management in acute lung injury secondary to septic shock. Chest 2009;136:102–109.

Nagdev A, Merchant R, Tirado-Gonzalez A, Sisson C, Murphy M. Emergency department bedside ultrasonographic measurement of the caval index for noninvasive determination of low central venous pressure. Ann Emerg Med 2010;55:290–295.

Nakamura K, Tomida M, Ando T, Sen K, Inokuchi R, Kobayashi E, Nakajima S, Sakuma I, Yahagi N. Cardiac variation of inferior vena cava: new concept in the evaluation of intravascular blood volume. J Med Ultrason (2001) 2013;40:205–209.

Otsu N. A threshold selection method from gray-level histograms. IEEE Transactions on Systems, Man and Cybernetics. Piscataway, NJ9: IEEE; 1979. p. 62–66.

Pasquero P, Albani S, Sitia E, Taulaigo A, Borio L, Berchialla P, Castagno F, Porta M. Inferior vena cava diameters and collapsibility index reveal early volume depletion in a blood donor model. Crit Ultrasound J 2015;7:17.

Sonoo T, Nakamura K, Ando T, Sen K, Maeda A, Kobayashi E, Sakuma I, Doi K, Nakajima S, Yahagi N. Prospective analysis of cardiac collapsibility of inferior vena cava using ultrasonography. J Crit Care 2015;30:945–948.

Zhang Z, Xu X, Ye S, Xu L. Ultrasonographic measurement of the respiratory variation in the inferior vena cava diameter is predictive of fluid responsiveness in critically ill patients: Systematic review and meta-analysis. Ultrasound Med Biol 2014;40:845–853.